



Published in final edited form as:

Surg Neurol. 2009 July ; 72(1): 20–35. doi:10.1016/j.surneu.2009.03.008.

Association of Chiari malformation type I and tethered cord syndrome: preliminary results of sectioning filum terminale[★]

Thomas H. Milhorat, MD^{a,*}, Paolo A. Bolognese, MD^a, Misao Nishikawa, MD, PhD^a, Clair A. Francomano, MD^b, Nazli B. McDonnell, MD, PhD^c, Chan Roonprapunt, MD, PhD^a, and Roger W. Kula, MD^a

^aDepartment of Neurosurgery, The Chiari Institute, Harvey Cushing Institutes of Neuroscience, North Shore-Long Island Jewish Health System, Manhasset, NY 11030, USA

^bHarvey Institute for Medical Genetics, Greater Baltimore Medical Center, Baltimore, MD 21204, USA

^cNational Institute on Aging, National Institutes of Health, Bethesda, MD 21224, USA

Abstract

Objective—The pathogenesis of CM-I is incompletely understood. We describe an association of CM-I and TCS that occurs in a subset of patients with normal size of the PCF.

Methods—The prevalence of TCS was determined in a consecutively accrued cohort of 2987 patients with CM-I and 289 patients with low-lying cerebellar tonsils (LLCT). Findings in 74 children and 244 adults undergoing SFT were reviewed retrospectively. Posterior cranial fossa size and volume were measured using reconstructed 2D computed tomographic scans and MR images. Results were compared to those in 155 age- and sex-matched healthy control individuals and 280 patients with generic CM-I. The relationships of neural and osseous structures at the CCJ and TLJ were investigated morphometrically on MR images. Intraoperative CDU was used to measure anatomical structures and CSF flow in the lumbar theca.

Results—Tethered cord syndrome was present in 408 patients with CM-I (14%) and 182 patients with LLCT (63%). In 318 patients undergoing SFT, there were no significant differences in the size or volume of the PCF as compared to healthy control individuals. Morphometric measurements demonstrated elongation of the brain stem (mean, 8.3 mm; $P < .001$), downward displacement of the medulla (mean, 4.6 mm; $P < .001$), and normal position of the CMD except in very young patients. Compared to patients with generic CM-I, the FM was significantly enlarged ($P < .001$). The FT was typically thin and taut (mean transverse diameter, 0.8 mm). After SFT, the cut ends of the FT distracted widely (mean, 41.7 mm) and CSF flow in the lumbar theca increased from a mean of 0.7 cm/s to a mean of 3.7 cm/s ($P < .001$). Symptoms were improved or resolved in 69 children (93%) and 203 adults (83%) and unchanged in 5 children (7%) and 39 adults (16%) and, worse, in 2 adults (1%) over a follow-up period of 6 to 27 months (mean, 16.1 months \pm 4.6 SD). Magnetic resonance imaging 1 to 18 months after surgery (mean, 5.7 months \pm 3.8 SD)

[★]This work was supported by the Research Foundation of the North Shore-Long Island Jewish Health System and the Intramural Research Program of the National Institutes of Health, National Institute on Aging.

*Corresponding author. Tel.: +1 516 562 3020; fax: +1 516 562 3030. milhorat@nshs.edu (T.H. Milhorat).

revealed upward migration of the CMD (mean, 5.1 mm, $P < .001$), ascent of the cerebellar tonsils (mean, 3.8 mm, $P < .001$), reduction of brain stem length (mean, 3.9 mm, $P < .001$), and improvement of scoliosis or syringomyelia in some cases.

Conclusions—Chiari malformation type I/TCS appears to be a unique clinical entity that occurs as a continuum with LLCT/TCS and is distinguished from generic CM-I by enlargement of the FM and the absence of a small PCF. Distinctive features include elongation and downward displacement of the hindbrain, normal position of the CMD, tight FT, and reduced CSF flow in the lumbar theca. There is preliminary evidence that SFT can reverse moderate degrees of tonsillar ectopia and is appropriate treatment for cerebellar ptosis after Chiari surgery in this cohort.

Keywords

Chiari malformation; Tethered cord; Filum terminale; Brain stem

1. Introduction

Chiari malformations comprise a heterogeneous group of hindbrain disorders that have in common herniation of the cerebellar tonsils through the FM. The type I deformity (CMI), defined as tonsillar herniation of 5 mm or greater [11], is encountered commonly in clinical practice. There is accumulating evidence that CM-I is a disorder of the paraxial mesoderm caused by underdevelopment of the PCF, overcrowding of the normally developed hindbrain, and downward displacement of the cerebellar tonsils [4,31,32,38,43,44,62,73]. The prevalence of CM-I is estimated to be in the range of 1 per 1000 to 1 per 5000 individuals [64]. Familial transmission can occur by autosomal recessive inheritance or autosomal dominant inheritance with incomplete penetrance, but most cases occur sporadically [38,64].

The impetus for this study was the identification of TCS in occasional patients referred for the evaluation of failed Chiari surgery before 2002. To examine a possible relationship of TCS and tonsillar herniation, we analyzed a consecutively accrued cohort of patients with CM-I to determine the incidence of the combined disorder. Clinical and radiographic findings were supplemented by morphometric measurements of the brain and spinal cord before and after SFT. The validity of criteria for the diagnosis of TCS was tested by surgical outcome data.

2. Clinical material and methods

2.1. Study population

The study population was composed of 2987 patients with MR imaging-confirmed CM-I and 289 patients with LLCT who were evaluated consecutively between January 2002 and July 2007. A total of 1507 patients (46%) had been referred for evaluation after failed Chiari surgery. There were 2488 female and 788 male patients who ranged in age from 1 to 88 years (mean age, 30.4 ± 4.0 years [\pm SD]). Children were defined as individuals between the ages of 0 to 18 years.

2.2. Assessment tools

A database (Microsoft Office Excel 2007) was established for each patient that included a detailed medical history and a checklist of symptoms and signs. Questionnaires were developed to elicit information on the family history, clinical features of CM-I, and clinical features of TCS. All patients underwent a physical examination, complete neurologic examination, whole-neuraxis MR imaging, CT of the head with 2D and 3D reconstruction, cine-MR imaging, and measurement of articular mobility. Additional information was provided in some patients by urodynamic testing, prone and vertical MR imaging, flexion and extension radiography of the cervical spine, CT scanning of the spine, barium swallow, 24-hour sleep monitoring, continuous cardiac monitoring, electrocardiography, echocardiography, tilttable testing, audiography, vestibular function tests, and neuropsychological assessments. The clinical disability of each patient was measured using the KPS, with scores ranging from 0 to 100 [39].

The clinical and radiographic/imaging criteria for establishing the diagnosis of CM-I have been described previously [38]. For the purposes of this study, we adopted the narrow but widely accepted definition of CM-I as tonsillar herniation of 5 mm or greater below the FM [11]. We defined MTH as tonsillar descent of 5 to 7 mm below the FM. Tonsillar descent of 0 to 4 mm was defined as LLCT.

The diagnosis of TCS was based on the following nonspecific but generally accepted symptoms and signs: urinary dysfunction (including incontinence, urgency, sensory loss, incomplete emptying of the bladder), bowel incontinence, low back pain, leg and foot pain, numbness of the soles of the feet, gait disturbance, leg weakness, atrophy of calf muscles, loss of deep tendon reflexes in the lower extremities, thoracolumbar scoliosis, equinovarus or equinovaglus deformities of the feet, and spinal dysraphism [2,10,18,28]. Traditional radiographic findings included evidence of a low-lying CMD below the lower endplate of L₂ and fatty infiltration or thickening (>2.0 mm diameter) of the FT [23]. In this study, we extended the radiographic criteria to include patients with the CMD positioned above the lower endplate of L₂ and absence of fatty infiltration or thickening of the FT, if patients evidenced classical symptomatology and met 5 or more of the following criteria: (1) neurogenic bladder confirmed by urodynamic testing, (2) positive toe walking test (relief of symptoms including low back pain and urinary urgency), (3) positive heel walking test (increase of symptoms including low back pain and urinary urgency), (4) positive pelvic traction and flexion test (increase of symptoms including low back pain and urinary urgency), (5) terminal thoracic syringomyelia (T₅ or below) in the absence of a rostral cavity, (6) thoracolumbar scoliosis [20,77], (7) spina bifida occulta, and (8) dorsal position of the FT on prone or vertical MR imaging.

2.3. Morphometric and volumetric analysis of the PCF

All morphometric measurements and volumetric calculations in this study were made by a single experienced observer (MN) who was unaware of other study data to avoid interobserver variability, which can increase the coefficient of error to more than 5% [8]. The results were reviewed independently by two experienced observers, who oversaw the process and verified all calculations. Using reconstructed 2D CT and MR imaging, the size

of the occipital bone was determined by measuring its enchondral components (exocciput, basiocciput, and supraocciput) which enclose the PCF [31,32,43,46]. Patients were excluded if they were 15 years of age and younger, or older than 69 years, to eliminate age-related changes of the skull and brain [63]. We measured the axial length of the clivus (basiocciput and basisphenoid) from the top of the dorsum sella to the basion; the axial length of the supraocciput from the center of the internal occipital protuberance to the opisthion; the axial length of the occipital condyle (exocciput) from the top of the jugular tubercle to the bottom of the occipital condyle [40,43,46]; and the widths of the clivus (distance between the bilateral carotid canals), supraocciput (distance between the inner surfaces of the asterions), and occipital condyle (distance between the outer surfaces of the condyles). We measured the anterior-posterior diameter of the FM between the inner surfaces of the basion and opisthion and its greatest inner transverse diameter (width). Radiographic analysis software (Image J, National Institutes of Health, Bethesda, MD) was used to calculate the surface area of the FM. The results were compared to those in 75 age- and sex-matched healthy control individuals.

The PCFV, PFBV, and PCF CSF volume were calculated on reconstructed 2D CT images using the Cavalieri method [8,33,38,51] or radiographic analysis software (Image J). The PCF was defined as the nearly spherical space bounded by the tentorium, occipital bone, clivus, and petrous bone [38,43]. The ridges of the petrous bone form the anterolateral border of the PCF and their connection to the posterior clinoids (posterior petroclinoid ligament) forms the anterior border. Volumetric calculations were compared to those in 75 age- and sex-matched healthy control individuals.

2.4. Morphometric analysis of the TLJ and CCJ

Neural and osseous relationships at the TLJ were investigated using MR imaging. The position of the CMD was measured as the distance between the plane of the upper endplate of L₁ and the tip of the conus on midsagittal T2-weighted images (Fig. 1A). In rare instances in which the FT could be identified clearly by fat signal, its transverse diameter was measured at L₄ on T1-weighted axial MR images.

Brain and bone structures comprising the PCF were investigated using T1-weighted MR images in the midsagittal plane (Fig. 1B). The cervicomedullary junction was identified radiologically by the inferior margin of the gracile tubercle [50]. We assessed brain and bone relationships using new measurements developed by us. The BSL was measured from the mesencephalic-pontine junction to the posterior-inferior margin of the gracile tubercle. We measured the MH from the pontomedullary junction to the FM along a line drawn perpendicular to McRae's line. The 4VH was measured as the perpendicular distance between Twining's line and the posterior apex of the fourth ventricle. For purposes of redrawing McRae's line after suboccipital craniectomy, the length of a line perpendicular to Twining's line and extending from the internal occipital protuberance to McRae's line was measured on preoperative films (Fig. 2A). The extent of cerebellar TH was measured from the tip of the cerebellar tonsils, or the tip of the more descended tonsil, to the McRae's line [37]. MR imaging was repeated 1 to 18 months postoperatively (mean, 5.7 months \pm 3.8

[\pm SD]), and morphometric findings before and after SFT were compared with 155 age- and sex-matched healthy control individuals.

2.5. Surgical technique

Operations were performed under general anesthesia and continuous SSEP and EMG monitoring. All patients were positioned prone on a standard, nonflexible operating table with bolsters under the shoulders and hips that maintained some degree of lumbar lordosis. An L₄ laminectomy was performed after localizing the correct level with a cross-table lateral x-ray or fluoroscopy. Using CDU, intrathecal structures were imaged between L₃ and L₅ and the transverse diameter of the FT was measured at L₄ on magnified images. CSF flow was measured as described elsewhere [36]. Thereafter, the dura was opened, the cauda equina and FT were mapped with a nerve stimulator, and the FT was sectioned after coagulating a short segment (2–4 mm) with bipolar forceps. The dura was closed with continuous, locking sutures of 5-0 Gore-Tex, and repeat CDU measurements were made. Before closing the wound, the patient was placed in extreme reverse Trendelenburg position, and a series of Valsalva maneuvers was performed. Cerebrospinal fluid leaks through stitch holes or ectatic dura were reinforced with thin strips of autogenous paraspinal muscle or fascia sewn in place with interrupted sutures of 5-0 Gore-Tex using an outer layer suturing technique. The dura was covered with a blood patch and the wound was closed.

2.6. Statistical analyses

Statistical analyses of clinical data were performed with SPSS for Macintosh (version 13.0 SPSS Inc, Chicago, Ill). Mean values are presented as \pm SDs. The incidence of associated clinical and radiographic findings was assessed using independent Student *t* tests. Categorical data were analyzed using 2 \times 2 contingency tables from which χ^2 were calculated and the corresponding *P* values were established. Analyses of morphometric data were performed with SPSS for Macintosh (version 13.0 SPSS, Inc). Demographic differences between patients and healthy control individuals were tested with the nonparametric Mann-Whitney *U* test. Comparisons of data before and after surgery were tested with rANOVA (repeated analysis of variants). The distribution of the data was analyzed using the *F* test. Significance was indicated by a 2-tailed probability value of less than .05.

3. Results

3.1. Prevalence of CM-I/TCS and LLCT/TCS

Four hundred eight of 2987 patients with CM-I (14%) and 182 (63%) of 289 patients with LLCT met the diagnostic criteria defined here for TCS. The criteria were tested by intraoperative findings and surgical outcome data in 318 patients undergoing SFT.

3.2. Characteristics of patients

The characteristics of patients undergoing SFT are shown in Table 1. Fourteen patients were identified through the Clinical and Molecular Manifestation of Hereditary Disorders of Connective Tissue Protocol (IRB Project 2003-086) at the National Institute on Aging. There were 74 children and 244 adults who ranged in age from 12 months to 60 years (mean age, 29.5 years \pm 4.1 [\pm SD]). Female patients outnumbered male patients by a ratio of 4:1.

One hundred fifty-three patients (48%) had been referred for evaluation of failed CM surgery. There were 49 first-degree relatives in 19 families who underwent SFT for CM-I/TCS or LLCT/TCS. All but 2 families appeared to have descended through the maternal lineage. It is likely that the number of affected relatives is underrepresented since one or more first-degree relatives in 92 additional families have a positive clinical diagnosis of CM-I/TCS or LLCT/TCS that has not been validated by SFT.

3.3. Clinical presentation of patients

The diagnostic findings in 74 children and 244 adults undergoing SFT are given in Table 2. The clinical presentation of the 2 age groups was similar except for an increased incidence of pelvic numbness ($P < .001$), low back pain ($P < .01$), interscapular pain ($P < .001$), paraesthesias of the hands and feet ($P < .01$), and arm pain or numbness ($P < .01$) in adults, and an increased incidence of pes cavus deformity ($P < .01$), urinary disturbances ($P < .01$), and ADHD ($P < .001$) in children. The diagnosis of ADHD was considered positive only if it had been made by a psychiatrist or clinical psychologist.

Sixty-three children (85%) and 217 adults (89%) met the diagnostic criteria for CM-I. The remainder had LLCT. The incidence of TH extending 8 mm or more below the FM was greater in children than adults (65% compared with 48%, $P < .05$, respectively), and the incidence of MTH was less in children than adults (20% compared with 41%, $P < .01$, respectively). The incidence of cervicothoracic, holocord, and terminal thoracic syringomyelia was similar in the 2 age groups. Thoracolumbar scoliosis, defined as trunk rotation equal to or greater than a Cobb angle of 15° [20,77], was more prevalent in children than adults (32% compared with 19%, $P < .05$, respectively).

The position of the CMD was assessed on sagittal MR images after counting the number of lumbar vertebral bodies on plain x-rays. Lumbarization of S_1 was present in 8 children (11%) and 18 adults (7%). The tip of the CMD was positioned above the lower end plate of L_2 in 300 of 318 patients (94%). There was a greater incidence of low position of the CMD in children than adults (19% compared with 2%, $P < .001$, respectively). Urodynamic testing revealed a greater incidence of neurogenic bladder in children than adults (76% compared with 53%, $P < .001$, respectively).

Patients with failed Chiari surgery had a varied clinical presentation but typically gave a history of postoperative improvement for several months after which symptoms returned and sometimes worsened. Of 153 patients, 95 (62%) had undergone additional surgical procedures including 1 or more PCF revisions (79 patients), CSF shunts (22 patients), and cranioplasty (9 patients) with suboptimal results. The most distinctive radiological finding was cerebellar ptosis with persistent TH and impaction of the FM (96 patients, 63%). Fifty-one patients (33%) had a cerebellar hernia extending through the cranial defect. There were no significant differences in the incidence of cerebellar ptosis or hernia in children as compared to adults.

3.4. Morphometric and volumetric analysis of the PCF

As shown in Table 3, patients with generic CM-I evidenced significant reductions in occipital bone size, PCFV, PCF CSF volume, and size of the FM as compared to healthy

control individuals ($P < .001$). There were no significant differences in occipital bone size, PCFV, and PCF CSF volume in patients with CM-I/TCS or LLCT/TCS. The size of the FM, measured as the anterior-posterior and transverse diameters and calculated as area (mm^2), was significantly enlarged in patients with CM-I/TCS and LLCT/TCS as compared to healthy control individuals.

3.5. Morphometric analysis of the TLJ and CCJ

The morphometric relationships of osseous and neural structures at the TLJ and CCJ are given in Table 4. In healthy control individuals, the position of the CMD, measured as the distance between the upper endplate of L_1 and the tip of the CMD (see Fig. 1A), moved rostrally by arithmetic progression during growth and development from a mean of $28.2 \text{ mm} \pm 8.9 \text{ SD}$ at 0 to 3 years of age to a mean of $21.2 \pm 11.8 \text{ SD}$ at maturity. There were no significant differences in the position of the CMD in patients with CM-I/TCS, LLCT/TCS, and healthy control individuals after the age of 8 years, although the measurements had large SDs that are common to normal distribution curves [60]. In patients between the ages of 0 and 7 years, the position of the CMD was low as compared to healthy control individuals (mean, 28.3 and 23.1 mm, $P < .01$, respectively). The FT could be identified reliably by MR imaging in only 9 children (12%) and 20 adults (9%).

The BSL, measured as the distance between the mesencephalic-pontine junction and the posterior-inferior margin of the gracilis tubercle, was greater in patients with CM-I/TCS and LLCT/TCS as compared to healthy control individuals in all age groups (mean, 8.3 mm, $P < .001$). The extent of brain stem elongation was greater in children than adults (mean, 10.1 and 5.5 mm, $P < .001$, respectively). We excluded assessments in 9 of 74 children (12%) and 35 of 244 adults (14%) in whom the inferior margin of the gracilis tubercle could not be identified reliably.

There were no significant differences in the extent of tonsillar herniation in children and adults. The MH was reduced by a mean of 4.6 mm ($P < .001$), and the distance of the fourth ventricle below Twining's line was increased by a mean of 4.2 mm ($P < .001$) as compared to healthy control individuals. Reductions of the MH and increases in the distance of the fourth ventricle below Twining's line were taken as evidence of downward displacement of the hindbrain in the absence of a short clivus and short supraocciput. These abnormalities tended to be pronounced in patients who developed cerebellar ptosis after Chiari decompression surgery (Fig. 2B).

3.6. Intraoperative CDU measurements

The dorsal dura between L_3 and L_5 was typically thin and semitransparent with a midline area of ectasia that resembled a wear track (Fig. 3A). The FT was identified on magnified axial CDU images and appeared as a thin, taut midline structure that was positioned posteriorly immediately beneath the overlying dura (Fig. 3B). Most fila had a weak or absent signal for fat and exhibited restricted or absent movements with respirations. No fila evidenced a central canal. The width of the FT, measured as its transverse diameter, varied from 0.4 to 3.2 mm and decreased steadily during growth and development from a mean of 1.8 mm between the ages of 0 to 3 years to a mean of 0.8 mm at maturity ($P < .01$). The

cauda equina tended to be arranged in tightly packed lateral bundles against the overlying dura and exhibited restricted movements with respirations. After SFT (Fig. 3C), the roots of the cauda equina were more evenly arranged and exhibited vigorous movements with respirations. The divided ends of the FT separately widely (mean distance, 41.7 mm \pm 3.1 SD). This magnitude of distraction was out of proportion to the coagulated segment and seemed to correlate with a visualized snap and brisk retraction at the moment of sectioning. The distracted ends of sectioned fila did not remain in a posterior position and fell limply into the ventral subarachnoid space (Fig. 4). In 25 patients (8%) in whom the diameter of the FT was 2 mm or greater, the divided ends retracted less briskly and were separated by shorter distances varying from 9 to 21 mm.

Color Doppler ultrasonography measurements of CSF flow were made transdurally before and after SFT. Before SFT, measurable CSF flow was confined mainly to the ventral subarachnoid space. The flow characteristics consisted of a mean peak velocity of 0.7 cm/s (\pm 0.6 SD), bidirectional movement, low power, high resistance, and a waveform exhibiting vascular variations (Fig. 3D). After SFT, measurable CSF flow was typically present in the dorsal and ventral subarachnoid spaces and in multiple streams between individual nerve roots and had the following characteristics: a mean peak velocity of 3.7 cm/s (\pm 1.4 SD), bidirectional movement, high power, low resistance, and a waveform exhibiting vascular and respiratory variations (Fig. 3E). The increase of CSF flow velocity after SFT was statistically significant ($P < .001$).

3.7. Surgical outcome

Table 5 summarizes outcome data in 318 patients undergoing SFT over a follow-up period of 6 to 27 months (mean, 16.1 \pm 4.6 months [\pm SD]). Spinal cord retethering occurred in 2 children, one of whom had dense lumbar arachnoiditis from a prior lumboperitoneal shunt. Complications in adult patients included wound infection (3 patients), CSF leak (2 patients), lumbar spine instability (1 patient), and epidural hematoma (1 patient). The unusually low incidence of CSF leaks in this series (0.6%) was felt to be a direct function of the surgical techniques used to repair thin or ectatic dura and for sealing stitch holes.

Before untethering surgery, a posterior fossa decompression or revision had been performed in 69 patients (22%), including 34 patients with tonsillar herniation below C₁ and 45 patients with complications of Chiari surgery. Surgical outcome and postoperative assessments in these patients may have been influenced by either or both procedures and cannot be attributed solely to the effects of untethered surgery.

Presenting symptoms and signs were improved in 69 (93%) of 74 children and 203 of 244 adults (83%), unchanged in 5 children (7%) and 39 adults (16%), and worse in 2 adults (1%). A complete resolution of symptoms occurred more frequently in children than adults (36% compared to 18%, $P < .001$, respectively). The comparatively small number of patients in whom symptoms resolved completely appeared to be related to the coexistence of TCS and hindbrain herniation, comorbidities such as syringomyelia and scoliosis, and the consequences of prior surgical treatment. In general, symptoms that tended to resolve in the immediate postoperative period included numbness and burning of the soles of the feet, leg pain, urinary disturbances, pelvic numbness, interscapular pain, paraesthesias of the hands,

and low back pain once surgical pain had subsided. Other symptoms such as neck pain, suboccipital headaches, and dizziness tended to improve over weeks or months. At follow-up, 11 (65%) of 17 children and 1 (33%) of 3 adults with ADHD had improved sufficiently that medications had been reduced or discontinued by the treating physician.

Terminal thoracic syrinxes resolved or were smaller in 20 (87%) of 23 children and 35 (65%) of 54 adult patients after SFT (Fig. 5). In contrast, cervicothoracic and holocord syrinxes did not resolve completely in either age group, although there was a 20% or greater reduction in the length and/or diameter of cavities in 9 (50%) of 18 children and 12 (28%) of 43 adults. Thoracolumbar scoliosis resolved or was reduced to a Cobb angle of 10° or less in 16 (67%) of 24 children and 11 (23%) of 47 adult patients during the period of follow-up. In 187 patients with neurogenic bladder, urodynamic abnormalities resolved or improved in 52 children (93%) and 110 adults (84%). Complete resolution of urodynamic dysfunction was greater in children than adults (66% as compared to 17%, $P < .001$, respectively).

3.8. Postoperative assessments of the TLJ and CCJ

As shown in Table 6, morphometric assessments after SFT revealed upward migration of the CMD by a mean distance of 5.1 mm ($P < .001$). The extent of CMD ascent was greater in children than adults (mean, 7.7 mm compared with 4.8 mm, $P < .01$, respectively). Morphometric measurements of the CCJ revealed a reduction of BSL (mean, 3.9 mm, $P < .001$), increased MH (mean, 3.3 mm, $P < .001$), decreased TH (mean, 3.8 mm, $P < .001$), and decreased distance of the fourth ventricle below Twining's line (mean, 2.6 mm, $P < .01$). These changes were present in 69 children and 203 adult patients whose symptoms improved or resolved after SFT and in 6 adults whose symptoms were unchanged. Increases of MH and decreases of TH and the distance of the fourth ventricle below Twining's line were taken as evidence of upward migration of the brain stem and cerebellum (Fig. 6). Hindbrain ascent after SFT was associated with reduced impaction of the FM and reduced size of some cervicothoracic and holocord syrinxes (Fig. 7). In patients with cerebellar ptosis and persistent or recurrent tonsillar herniation after Chiari surgery, SFT for previously unrecognized TCS resulted typically in ascent of the hindbrain and reshaping of the ptotic cerebellum (Fig. 8).

4. Discussion

The relationship of spinal cord tethering and Chiari malformations has long attracted interest and speculation. Early investigators believed that Chiari malformation type II was caused by spinal cord traction occurring with spina bifida and myelomeningocele [3,14,29,45]. Lichtenstein [29] proposed that caudal fixation of the spinal cord in utero prevents the normal ascent of the neuraxis during growth and development, resulting in downward displacement of the cerebellum and brain stem through the FM. This cord traction theory was generally dismissed as an oversimplification that did not account for the complex neural and osseous anomalies of Chiari malformation type II [35,54] and did not explain why nerve roots below the mid-thoracic level coursed normally rather than cephalad as would be expected if there was significant downward traction on the CMD [6]. Unfortunately, there are no experimental models that test the cord traction theory directly. Techniques for

inducing neural tube defects, for example, introduce a wide variety of variables including hydrocephalus, myelomeningocele, caudal dislocation of the brain stem and cerebellum, hypoplasia of the PCF, and enlargement of the FM [9] that have more than one potential mechanism of tonsillar ectopia and are difficult to relate to CM-I. To date, lesions that tether the spinal cord have been reported only occasionally in association with CM-I including ten patients with lipomyelomeningocele [5,41,68,75], 4 patients with a “tight” FT [53], one patient with an intraspinal lipoma [49], and a 3 year-old girl with a thick fatty FT who exhibited increasing tonsillar herniation with somatic growth [1]. To date, there are no published reports of an explicit relationship between CM-I and TCS. In a recent study of spinal cord traction in fresh cadavers [71], caudal tension on the CMD was found to produce less than 1 mm downward movement of the medulla and upper cervical spinal cord and no displacement of the cerebellar tonsils. The authors concluded that caudal fixation of the spinal cord is an implausible cause of CM-I and that SFT is unlikely to reverse tonsillar ectopia.

Modern interest in TCS may be said to have been stimulated by Hoffman et al [18] who reported a series of 31 children with spina bifida occulta and elongated spinal cords in whom section of a fibrotic or lipomatous FT resulted in significant symptomatic improvement. The authors introduced the term *tethered spinal cord* to distinguish the disorder from more complex conditions such as myelomeningocele, lipomyelomeningocele, diastematomyelia, and intraspinal space-occupying dysraphic lesions such as dermoid tumors. In recent years, TCS has come to be recognized as a clinically important disorder in children and adults [2,16,17,21,27,28,48,74,80]. Anatomical abnormalities of the FT are thought to be due to disturbances of retrogressive differentiation during secondary neurulation that contribute to fibrofatty infiltration and reduced viscoelasticity [27,28,72,79]. The pathogenesis of the syndrome is attributed to downward traction on the CMD by a tight FT that results in stretching of neuronal elements [2,55,67], impaired regional blood flow [15,24,26,56] and a decrease of oxidative metabolism [81]. The symptomatology includes bladder and bowel disturbances, back and leg pain, lower extremity weakness, and segmental sensory disturbances [2,10,17,28]. The traditional diagnosis of TCS has required radiographic evidence of a short, thick or fatty FT and a lowlying CMD with its tip positioned at or below the lower endplate of L₂ [23,48,59,65,74,78,82]. The syndrome is associated with an increased incidence of terminal thoracic syringomyelia [7,12,22].

The possibility that TCS can occur in patients with normal position of the CMD was first proposed by Warden and Oakes [74]. In 1990, Khoury et al [25], reported a series of 31 children with neurogenic bladder dysfunction and normal radiographic findings in whom SFT resulted in symptomatic improvement in 72% of the patients. Subsequent surgical series in children with TCS and a normally positioned CMD have described clinical or urodynamic improvements in 71% to 100% of the patients [34,42,47,57,58,61,74,76]. Growing interest in the concept of minimal or occult TCS has required a re-examination of the criteria for diagnosis and surgical intervention [59,66,72,80]. In a recent questionnaire-based survey of attendees at the Annual Meeting of the American Association of Neurological Surgeons (AANS)/Congress of Neurological Surgeons (CNS) Section on Pediatric Neurological Surgery in December, 2004, the responses revealed a high level of uncertainty concerning

the surgical indications for SFT in children with voiding disturbances when the CMD is positioned normally [65].

The controversial status of TCS posed a number of challenges for the current study. Because the diagnosis is inexact and often subjective, we relied on generally accepted clinical and radiographic criteria [2,10,18,23,28,42,52]. These criteria were supplemented by additional tests and a grading system to minimize subjectivity. Using this methodology, 408 (14%) of 2987 patients with CM-I and 182 (63%) of 289 patients with LLCT met the diagnostic criteria for TCS. To further validate the diagnosis, the reported results were limited to findings in 318 patients undergoing SFT so that intraoperative findings and surgical outcome data could be correlated. It is difficult to say whether entry requirements for this study broadened or narrowed the indications for untethering surgery since a number of patients were excluded, including those with a neurogenic bladder, if they did not meet a graded list of objective criteria.

Morphometric measurements of the PCF revealed major differences between patients with CM-I/TCS and LLCT/TCS and those with generic CM-I. In the latter cohort, there were significant reductions in occipital bone size, PCFV, and size of the FM as compared to healthy control individuals ($P < .001$). The findings were consistent with previously reported data, and support the generally held belief that CM-I is caused by underdevelopment of PCF and overcrowding of the hindbrain which are responsible for herniation of the cerebellar tonsils [4,31,32,38,43]. In patients with CM-I/TCS and LLCT/TCS, on the other hand, the occipital bone size was normal, the PCFV was normal, and the size of the FM was enlarged ($P < .001$) as compared to healthy control individuals. Absence of a small PCF would appear to exclude hindbrain overcrowding as the proximate cause of tonsillar herniation and suggests that CM-I/TCS represents a distinct clinical entity that can be differentiated radiographically from generic CM-I. In a morphometric analysis of the PCF in children, Tubbs et al [69] reported evidence of enlargement of the FM and caudal displacement of the brainstem in 6 patients with Chiari 0 malformation. The study did not include a volumetric assessment of the PCF. Subsequently, the authors reported normal PCF volumes in patients with CM-I and lipomyelomeningocele [68] and have recently described a family with four generations of CM-I in which all members had a normal PCFV [70]. The similarities of these cases to those in the current study suggest that some may have been associated with occult spinal cord tethering. Enlargement of the FM under these circumstances is consistent with a process that occurs early in development before the basioccipital and spheno-occipital sutures are well formed [13,19,30].

In 318 patients with CM-I/TCS or LLCT/TCS, the symptomatology of spinal cord tethering tended to be subordinated to that of TH and associated abnormalities. Traditional radiographic criteria such as low position of the CMD applied to only a small minority of patients. The most reliable diagnosis of TCS was made by morphometric assessments of the CCJ rather than the TLJ. In particular, in all patients with a favorable response to SFT ($n = 272$), there was evidence of brain stem elongation and downward displacement of the hindbrain as reflected by a decreased MH and an increased distance of the fourth ventricle below Twining's line. There were 6 adult patients whose condition did not improve after

SFT. The reliability of morphometric assessments for predicting short-term surgical outcome was 98%.

The difficulties of diagnosing TCS radiographically were evident at surgery. Typically, the FT was positioned dorsally against the overlying dura, had weak or absent signal for fat, and measured less than 1 mm in transverse diameter. These features are at the lower ranges of MR imaging resolution. The dura overlying the FT was typically thin and semitransparent (see Fig. 3A). Although there was no methodology to measure mechanical tension, the FT appeared taut and vibrated like a guitar string when plucked through the dura. Other findings that were consistent with tightness of the FT included restricted or absent movements with respirations, lateral packing of the cauda equina (see Fig. 3B), and reduced velocity of CSF flow in the lumbar theca (see Fig. 3D), possibly as a consequence of decreased neural movements. The term *occult TCS* was felt to be particularly apt for a disorder characterized by clinical features of TCS, normal position of the CMD, and an FT that is difficult to identify by MR imaging.

As pointed out by many authors, the pathophysiology of occult TCS has been difficult to understand given the absence of a low-lying CMD [2,28,61,65,66,72,80]. Histological studies have suggested that fila obtained from patients with occult TCS may be more fibrotic than normal [58,61,78], lending support to the notion that a normally positioned CMD could be tethered by a tight or inelastic FT [60,66,72,78]. This hypothesis is supported by the following findings in the current report: [1] the width of the FT decreased steadily as the CMD ascended during growth and development; [2] most patients with normal position of the CMD had positive FT traction tests; [3] at surgery, the FT appeared as a thin, taut, immobile structure that was associated with lateral packing of the cauda equina and reduced regional CSF flow; and [4] immediately after SFT, there was marked distraction of the divided ends, normalized distribution and movements of the cauda equina and increased regional CSF flow (see Fig. 3C and E). Because CMD blood flow was not measured, we could not confirm that abnormalities are present [56,81] or whether changes occur after SFT.

The most unexpected consequence of SFT was morphometric evidence of upward migration of the CMD (mean, 5.1 mm, $P < .001$), reduction of BSL (mean, 3.9 mm, $P < .001$), ascent of the cerebellar tonsils (mean, 3.8 mm, $P < .001$), and ascent of the medulla (mean, 3.3 mm, $P < .001$) (see Fig. 6). In some cases, these changes were accompanied by an improvement of scoliosis or syringomyelia (see Fig. 7). Because MR imaging was performed 1 to 18 months after surgery (mean, 5.7 months \pm 3.8 [\pm SD]), the extent of long-term changes and the interval over which they occur have not been established.

The key question raised by these findings is how can traction from below account for tonsillar ectopia in patients whose CMD is in a normal position? The phenomenon on its surface appears contradictory. Lacking a direct way to measure tension in the filum and neural tissues, we relied on circumstantial evidence. Intraoperative observations were made with the patient prone on a standard operating table with bolsters under the shoulders and hips that maintained some degree of lumbar lordosis. Under these conditions, the filum was found in a posterior position immediately beneath the overlying dura. The dorsal midline dura was characteristically thin and ectatic resembling a wear tract. When seen through the

dura or after opening dura, the filum was abnormally thin (0.8 mm mean diameter), appeared tight to experienced eyes, did not move with respirations, and vibrated when manipulated. Upon sectioning, the filum snapped and retracted briskly with the cut ends falling limply into the ventral subarachnoid space (see Fig. 4). Intraoperative CDU imaging revealed a significant increase in CSF flow and increased movements of the cauda equina after sectioning (see Fig. 3). Despite normal position of the CMD as defined by standard radiographic criteria, postoperative morphometric measurements demonstrated that it had migrated cephalad to a new position significantly above its original position. Our working hypothesis is that the association of CM-I and TCS is explained by a tight and inelastic FT. If the FT is extremely tight, as in the case of patients with thick fatty fila, the conus is anchored and remains below the lower endplate of L₂. On the other hand, if the FT is sufficiently elastic, it can stretch with somatic growth allowing the conus to ascend to a position assumed to be normal while maintaining varying degrees of pathological tension. The best evidence for this is that the conus ascends after SFT accompanied by ascent of the hindbrain and normalization of brain stem length. Such a hypothesis could embrace a continuum of abnormally tight fila having varying degrees of thickness and tension that result in varying positions of the CMD and hindbrain.

From a diagnostic standpoint, we believe that occult spinal cord tethering should be suspected in any patient with CM-I or LLCT who has TCS-like symptoms that are accompanied by positive FT traction tests, terminal thoracic syringomyelia, thoracolumbar scoliosis, or cerebellar ptosis after Chiari decompression surgery. The disorder should probably be added to the differential diagnosis of ill-defined conditions such as idiopathic scoliosis, behavioral disturbances in children, delayed toilet training, low back pain, restless legs syndrome, and genitourinary dysfunction in adults. The most reliable diagnosis of occult TCS in this study was made by morphometric measurements showing elongation and downward displacement of the hindbrain on MR imaging scans of the brain and cervical spine.

Optimal strategies for the management of patients with CM-I/TCS have yet to be determined. Based on our current experience, we do not perform and do not recommend untethering surgery in patients with normal position of the CMD unless there is evidence of brainstem elongation, downward displacement of the medulla, and low position of the fourth ventricle. In patients with large tonsillar herniations extending below the arch of C₁, it is our practice to perform a posterior fossa decompression before SFT to avoid the potential risk of exacerbating tonsillar herniation by the sudden release of lumbar CSF. Untethering is then performed as a staged procedure. In all other patients, untethering is performed as the primary procedure, and the patients are followed for evidence of tonsillar ascent symptomatic improvement over an indeterminate period of time. Most of the patients in this latter subset are currently improved and no longer meet our indications for Chiari surgery [36], but longer follow-up is obviously required. The observations in this retrospective report will need to be confirmed by prospective, randomized, carefully controlled studies that are capable of providing Class I evidence.

5. Conclusions

An association of CM-I and TCS is described that mimics generic CM-I but is distinguished from it by the presence of a normally sized PCF. Typically, the FT is thin and taut and the CMD is positioned above the lower endplate of L₂. TCS was found to be accompanied by varying degrees of tonsillar herniation and was particularly common in patients with LLCT. Associated abnormalities included cerebellar ptosis in patients with failed Chiari surgery, terminal thoracic syringomyelia, and idiopathic scoliosis. The most reliable diagnosis of occult spinal cord tethering was made by morphometric evidence of brain stem elongation, downward displacement of the hindbrain, and enlargement of the FM. The absence of a hypoplastic PCF and the presence of an enlarged FM are consistent with cord-traction as the proximate cause of tonsillar ectopia. The apparently contradictory phenomenon of a normally positioned CMD may be explained by variations in the elasticity and plasticity of the tight FT which allow the conus to ascend with somatic growth while maintaining some degree of pathological tension. Simple SFT may be effective in relieving symptomatology, restoring normal brain stem length, normalizing the position of the cerebellar tonsils, and, in many cases, avoiding the need for posterior fossa surgery.

Acknowledgments

The authors thank Dr Raymond V. Damadian (Fonar Corporation) for providing technical assistance and supervision of patients undergoing vertical MRI.

Abbreviations

4VH	height of the fourth ventricle
ADHD	attention deficit hyperactivity disorder
BSL	axial length of the brain stem
CCJ	craniovertebral junction
CDU	color Doppler ultrasonography
CM-I	Chiari malformation type I
CMD	conus medullaris
CSF	cerebrospinal fluid
CT	computed tomography
EMG	electromyography
FM	foramen magnum
FT	filum terminale
KPS	Karnofsky Performance Scale
LLCT	low-lying cerebellar tonsils

MH	height of the medulla
MR	magnetic resonance
MTH	minimal tonsillar herniation
PCF	posterior cranial fossa
PCFV	posterior cranial fossa volume
PFBV	posterior cranial fossa brain volume
SFT	section of the FT
SSEP	somatosensory evoked potential
TCS	tethered cord syndrome
TLJ	thoracolumbar junction
TH	tonsil herniation

References

1. Abel TJ, Chowdhary A, Gabikian P, Ellenbogen RG, Avellino AM. Acquired chiari malformation type I associated with a fatty terminal filum. Case report. *J Neurosurg.* 2006; 105:329–32. [PubMed: 17328286]
2. Agarwalla PK, Dunn IF, Scott RM, Smith ER. Tethered cord syndrome. *Neurosurg Clin N Am.* 2007; 18:531–47. [PubMed: 17678753]
3. Alexander GL. Surgical lesions of spinal cord and nerve-roots (Honyman Gillespie lecture). *Edinburgh Med J.* 1942; 49:409–24.
4. Badie B, Mendoza D, Batzdorf U. Posterior fossa volume and response to suboccipital decompression in patients with Chiari I malformation. *Neurosurgery.* 1995; 37:214–8. [PubMed: 7477771]
5. Barami K, Pereira J, Canady AI. Anterolateral lumbar lipomyelomeningocele: case report and review of the literature. *Neurosurgery.* 1997; 41:1421–4. [PubMed: 9402597]
6. Barry A, Patten BM, Stewart BH. Possible factors in the development of the Arnold-Chiari malformation. *J Neurosurg.* 1957; 14:285–301. [PubMed: 13429397]
7. Beaumont A, Muszynski CA, Kaufman BA. Clinical significance of terminal syringomyelia in association with pediatric tethered cord syndrome. *Pediatr Neurosurg.* 2007; 43:216–21. [PubMed: 17409791]
8. Clatterbuck RE, Sipos EP. The efficient calculation of neurosurgically relevant volumes from computed tomographic scans using Cavalieri's Direct Estimator. *Neurosurgery.* 1997; 40:339–43. [PubMed: 9007867]
9. DiRocco C, Rende M. Neural tube defects. *Child's Nerv Syst.* 1987; 3:334–41. [PubMed: 3450385]
10. Drake JM. Occult tethered cord syndrome: not an indication for surgery. *J Neurosurg (5 Suppl Pediatrics).* 2006; 104:305–8.
11. Elster AD, Chen MY. Chiari I malformations: clinical and radiologic reappraisal. *Radiology.* 1992; 183:347–53. [PubMed: 1561334]
12. Erkan K, Unal F, Kiris T. Terminal syringomyelia in association with the tethered cord syndrome. *Neurosurgery.* 1999; 45:1351–60. [PubMed: 10598703]
13. Friede H. Normal development and growth of the human neurocranium and cranial base. *Scand J Plast Reconstr Surg.* 1981; 15:163–9. [PubMed: 7051266]

14. Fuchs A. Ueber Beziehungen der Enuresis nocturna zu Rudimetärformen der Spina bifida occulta (Myelodysplasie). *Wien Med Wochenschr.* 1910; 80:1569–73.
15. Fuse T, Patrickson JW, Yamada S. Axonal transport of horseradish peroxidase in the experimental tethered spinal cord. *Pediatr Neurosci.* 1989; 15:296–301. [PubMed: 2484977]
16. Gupta SK, Khosla VK, Sharma BS, Mathuriya SN, Pathak A, Tewari MK. Tethered cord syndrome in adults. *Surg Neurol.* 1999; 52:362–9. [PubMed: 10555842]
17. Hendrick EB, Hoffman HJ, Humphreys RP. The tethered spinal cord. *Clin Neurosurg.* 1983; 30:457–63. [PubMed: 6667586]
18. Hoffman HJ, Hendrick EB, Humphreys RP. The tethered spinal cord: its protean manifestations, diagnosis and surgical correction. *Childs Brain.* 1976; 2:145–55. [PubMed: 786565]
19. Hoyte DA. The cranial base in normal and abnormal skull growth. *Neurosurg Clin N Am.* 1991; 2:515–37. [PubMed: 1821300]
20. Huang SC. Cut-off point of the Scoliometer in school scoliosis screening. *Spine.* 1997; 22:1985–9. [PubMed: 9306527]
21. Huttman S, Krauss J, Collmann H, Sörensen N, Roosen K. Surgical management of tethered spinal cord in adults: report of 54 cases. *J Neurosurg.* 2001; 95:173–8. [PubMed: 11599833]
22. Iskandar BJ, Oakes WJ, McLaughlin C, Osumi AK, Tien RD. Terminal syringohydromyelia and occult spinal dysraphism. *J Neurosurg.* 1994; 81:513–9. [PubMed: 7931583]
23. Iskander, BJ., Oakes, WJ. Occult spinal dysraphism. In: Albright, AL, Pollack, IF., Adelson, PD., editors. *Principles and practice of pediatric neurosurgery.* New York: Thieme; 1999. p. 321-51.
24. Kang JK, Kim MC, Kim DS, Song JU. Effects of tethering on regional spinal cord blood flow and sensory-evoked potentials in growing cats. *Childs Nerv Syst.* 1987; 3:35–9. [PubMed: 3594467]
25. Khoury AE, Hendrick EB, McLorie GA, Kulkarni A, Churchill BM. Occult spinal dysraphism: clinical and urodynamic outcome after division of the filum terminale. *J Urol.* 1990; 144:426–9. [PubMed: 2197434]
26. Koçak A, Kiliç A, Nurlu G, Konan A, Kiliç K, Cirak B, Cirak B, Colak A. A new model for tethered cord syndrome: a biochemical, electrophysiological, and electron microscopic study. *Pediatr Neurosurg.* 1997; 26:120–6. [PubMed: 9419028]
27. Lapsiwala SB, Iskandar BJ. The tethered cord syndrome in adults with spina bifida occulta. *Neurol Res.* 2004; 26:735–40. [PubMed: 15494114]
28. Lew SM, Kothbauer KF. Tethered cord syndrome: an updated review. *Pediatr Neurosurg.* 2007; 43:236–48. [PubMed: 17409793]
29. Lichtenstein BW. Distant neuroanatomic complications of spina bifida (spinal dysraphism). Hydrocephalus, Arnold-Chiari deformity, stenosis of the aqueduct of Sylvius, etc.; pathogenesis and pathology. *Arch Neurol Psychiat.* 1940; 47:195–214.
30. Madeline LA, Elster AD. Suture closure in the human chondrocranium: CT assessment. *Radiology.* 1995; 196:747–56. [PubMed: 7644639]
31. Marin-Padilla M. Notochordal-basichondrocranium relationships: abnormalities in experimental axial skeletal (dysraphic) disorders. *J Embryol Exp Morphol.* 1979; 53:15–38. [PubMed: 536685]
32. Marin-Padilla M, Marin-Padilla TM. Morphogenesis of experimentally induced Arnold-Chiari malformation. *J Neurol Sci.* 1981; 50:29–55. [PubMed: 7229658]
33. Mayhew TM, Olsen DR. Magnetic resonance imaging (MRI) and model-free estimates of brain volume determined using the Cavalieri principle. *J Anat.* 1991; 178:133–44. [PubMed: 1810922]
34. Metcalfe PD, Luerssen TG, King SJ, Kaefer M, Meldrum KK, Cain MP, Rink RC, Casale AJ. Treatment of the occult tethered spinal cord for neuropathic bladder: results of sectioning the filum terminale. *J Urol.* 2006; 176:1826–30. [PubMed: 16945660]
35. Milhorat, TH. Hydrocephalus and the cerebrospinal fluid. Baltimore: Williams & Wilkins Inc; 1972. p. 111-23.
36. Milhorat TH, Bolognese PA. Tailored operative technique for Chiari type I malformation using intraoperative color Doppler ultrasonography. *Neurosurgery.* 2003; 53:899–906. [PubMed: 14519223]

37. Milhorat TH, Bolognese PA, Nishikawa M, McDonnell NB, Francomano CA. Syndrome of occipitoatlantoaxial hypermobility, cranial settling, and Chiari malformation type I in patients with hereditary disorders of connective tissue. *J Neurosurg Spine*. 2007; 7:601–9. [PubMed: 18074684]
38. Milhorat TH, Chou MW, Trinidad EM, Kula RW, Mandell M, Wolpert C, Speer MC. Chiari I malformation redefined: clinical and radiographic findings for 364 symptomatic patients. *Neurosurgery*. 1999; 44:1005–17. [PubMed: 10232534]
39. Mor V, Laliberte L, Morris JN, Wiemann M. The Karnofsky Performance Status Scale. An examination of its reliability and validity in a research setting. *Cancer*. 1984; 53:2002–7. [PubMed: 6704925]
40. Muller F, O’Rahilly R. Occipitocervical segmentation in staged human embryos. *J Anat*. 1994; 185(Pt 2):251–8. [PubMed: 7961131]
41. Naidich TP, McLone DG, Fulling KH. The Chiari II malformation: part IV. The hindbrain deformity. *Neuroradiology*. 1983; 25:179–97. [PubMed: 6605491]
42. Nazar GB, Casale AJ, Roberts JG, Linden RD. Occult filum terminale syndrome. *Pediatr Neurosurg*. 1995; 23:228–35. [PubMed: 8688347]
43. Nishikawa M, Sakamoto H, Hakuba A, Nakanishi N, Inoue Y. Pathogenesis of Chiari malformation: a morphometric study of the posterior cranial fossa. *J Neurosurg*. 1997; 86:40–7. [PubMed: 8988080]
44. Nyland H, Krogness KG. Size of posterior fossa in Chiari type I malformation in adults. *Acta Neurochir (Wien)*. 1978; 40:233–42. [PubMed: 676804]
45. Ogryzlo MA. Arnold-Chiari malformation. *Arch Neurol Psychiat*. 1942; 48:30–46.
46. O’Rahilly R, Muller F, Meyer DB. The human vertebral column at the end of the embryonic period proper. 2. The occipitocervical region. *J Anat*. 1983; 136:181–95. [PubMed: 6833119]
47. Palmer JS, Maizels M, Grant JA, Richards I, Kaplan WE. Transection of filum terminale remits urinary and stool continence in children with neuropathic bladder and spina bifida occulta. *Am Acad Pediatr*. 1999; 11 [Abstr].
48. Pang D, Wilberger JE Jr. Tethered cord syndrome in adults. *J Neurosurg*. 1982; 57:32–47. [PubMed: 7086498]
49. Pierre-Kahn A, Lacombe J, Pichon J, Giudicelli Y, Renier D, Sainte-Rose C, Perrigot M, Hirsch JF. Intraspinal lipomas with spina bifida. Prognosis and treatment in 73 cases *J Neurosurg*. 1986; 65:756–61. [PubMed: 3534161]
50. Press GA, Murakami J, Courchesne E, Berthoty DP, Grafe M, Wiley CA, Hesselink JR. The cerebellum in sagittal plane—atomic-MR correlation: 2. The cerebellar hemispheres. *AJR Am J Roentgenol*. 1989; 153:837–46. [PubMed: 2773741]
51. Regeur L, Pakkenberg B. Optimizing sampling designs for volume measurements of components of human brain using a stereological method. *J Microsc*. 1989; 155:113–21. [PubMed: 2769747]
52. Rinaldi F, Cioffi FA, Columbano L, Krasagakis G, Bernini FP. Tethered cord syndrome. *J Neurosurg Sci*. 2005; 49:131–5. [PubMed: 16374403]
53. Royo-Salvador MB, Sole-Llenas J, Domenech JM, González-Adrio R. Results of the section of the filum terminale in 20 patients with syringomyelia, scoliosis and Chiari malformation. *Acta Neurochir (Wien)*. 2005; 147:515–23. [PubMed: 15723156]
54. Russell, DS. Observation on the pathology of hydrocephalus. London: Her Majesty’s Stationery Office; 1949. p. 21–38.(Special Report Series Medical Research Council, no 265)
55. Sarwar M, Crelin ES, Kier EL, Virapongse C. Experimental cord stretchability and the tethered cord syndrome. *AJNR Am J Neuroradiol*. 1983; 4:641–3. [PubMed: 6410820]
56. Schneider SJ, Rosenthal AD, Greenberg BM, Danto J. A preliminary report on the use of laser-Doppler flowmetry during tethered spinal cord release. *Neurosurgery*. 1993; 32:214–8. [PubMed: 8437659]
57. Selçuki M, Unlü A, Uur HC, Soygür T, Arıkan N, Selçuki D. Patients with urinary incontinence often benefit from surgical detethering of tight filum terminale. *Childs Nerv Syst*. 2000; 16:150–5. [PubMed: 10804050]
58. Selçuki M, Vatanserver S, Inan S, Erdemli E, Bado lu C, Polat A. Is a filum terminale with a normal appearance really normal? *Childs Nerv Syst*. 2003; 19:3–10. [PubMed: 12541079]

59. Selden NR. Occult tethered cord syndrome: the case for surgery. *J Neurosurg (5 Suppl Pediatrics)*. 2006; 104:302–4.
60. Selden NR. Minimal tethered cord syndrome: what's necessary to justify a new surgical indication? *Neurosurg Focus*. 2007; 23(2):E1.
61. Selden NR, Nixon RR, Skoog SR, Lashley DB. Minimal tethered cord syndrome associated with thickening of the terminal filum. *J Neurosurg (3 Suppl Pediatrics)*. 2006; 105:214–8.
62. Schady W, Metcalfe RA, Butler P. The incidence of craniocervical bony anomalies in the adult Chiari malformation. *J Neurol Sci*. 1987; 82:193–203. [PubMed: 3440866]
63. Schaefer GB, Thompson JN Jr, Bodensteiner JB, Gingold M, Wilson M, Wilson D. Age-related changes in the relative growth of the posterior fossa. *J Child Neurol*. 1991; 6:15–9. [PubMed: 2002195]
64. Speer MC, George TM, Enterline DS, Franklin A, Wolpert CM, Milhorat TH. A genetic hypothesis for Chiari I malformation with or without syringomyelia. *Neurosurg Focus*. 2000; 8(3):E12. [PubMed: 16676924]
65. Steinbok P, Garton HJ, Gupta N. Occult tethered cord syndrome: a survey of practice patterns. *J Neurosurg (5 Suppl Pediatrics)*. 2006; 104:309–13.
66. Steinbok P, MacNeily AE. Section of the terminal filum for occult tethered cord syndrome: toward a scientific answer. *Neurosurg Focus*. 2007; 23(2):E5.
67. Tani S, Yamada S, Knighton RS. Extensibility of the lumbar and sacral cord. Pathophysiology of the tethered spinal cord in cats. *J Neurosurg*. 1987; 66:116–23. [PubMed: 3783242]
68. Tubbs RS, Bui CJ, Rice WC, Loukas M, Naftel RP, Holcombe MP, Oakes WJ. Critical analysis of the Chiari malformation type I found in children with lipomyelomeningocele. *J Neurosurg*. 2007; 106:196–200.
69. Tubbs RS, Elton S, Grabb P, Dockery SE, Bartolucci AA, Oakes WJ. Analysis of the posterior fossa in children with the Chiari 0 malformation. *Neurosurgery*. 2001; 48:1050–5. [PubMed: 11334271]
70. Tubbs RS, Hill M, Loukas M, Shoja MM, Oakes WJ. Volumetric analysis of the posterior cranial fossa in a family with four generations of the Chiari malformation type I. *J Neurosurg Pediatrics*. 2008; 1:21–4.
71. Tubbs RS, Loukas M, Shoja MM, Oakes WJ. Observations at the craniocervical junction with simultaneous caudal traction of the spinal cord. *Childs Nerv Syst*. 2007; 23:367–9. [PubMed: 17203326]
72. Tubbs RS, Oakes WJ. Can the conus medullaris in normal position be tethered? *Neurol Res*. 2004; 26:727–31. [PubMed: 15494112]
73. Vega A, Quintana F, Berciano J. Basichondrocranium anomalies in adult Chiari type I malformation: a morphometric study. *J Neurol Sci*. 1990; 99:137–45. [PubMed: 2086722]
74. Warder DE, Oakes WJ. Tethered cord syndrome and the conus in a normal position. *Neurosurgery*. 1993; 33:374–8. [PubMed: 8413866]
75. Waldau B, Grant G, Fuchs H. Development of an acquired Chiari malformation type I in the setting of an untreated lipomyelomeningocele. Case report. *J Neurosurg Pediatrics*. 2008; 1:164–6.
76. Wehby MC, O'Hollaren PS, Abtin K, Hume JL, Richards BJ. Occult tight filum terminale syndrome: results of surgical untethering. *Pediatr Neurosurg*. 2004; 40:51–7. [PubMed: 15292632]
77. Whittle MW, Evans M. Instrument for measuring the Cobb angle in scoliosis. *Lancet*. 1979; 1:414. [PubMed: 84265]
78. Wilson DA, Prince JR. MR imaging determination of the location of the normal conus medullaris throughout childhood. *AJR Am J Roentgenol*. 1989; 152:1029–32. [PubMed: 2650477]
79. Yamada S, Won DJ, Pezeshkpour G, Yamada BS, Yamada SM, Siddiqi J, Zouros A, Colohan AR. Pathophysiology of tethered cord syndrome and similar complex disorders. *Neurosurg Focus*. 2007; 23(2):E6.
80. Yamada S, Won DJ, Yamada SM, Hadden A, Siddiqi J. Adult tethered cord syndrome: relative to spinal cord length and filum thickness. *Neurol Res*. 2004; 26:732–4. [PubMed: 15494113]
81. Yamada S, Zinke DE, Sanders D. Pathophysiology of "tethered cord syndrome". *J Neurosurg*. 1981; 54:494–503. [PubMed: 6259301]

82. Yundt KD, Park TS, Kaufman BA. Normal diameter of filum terminale in children: in vivo measurement. *Pediatr Neurosurg.* 1997; 27:257–9. [PubMed: 9620003]

Author Manuscript

Author Manuscript

Author Manuscript

Author Manuscript

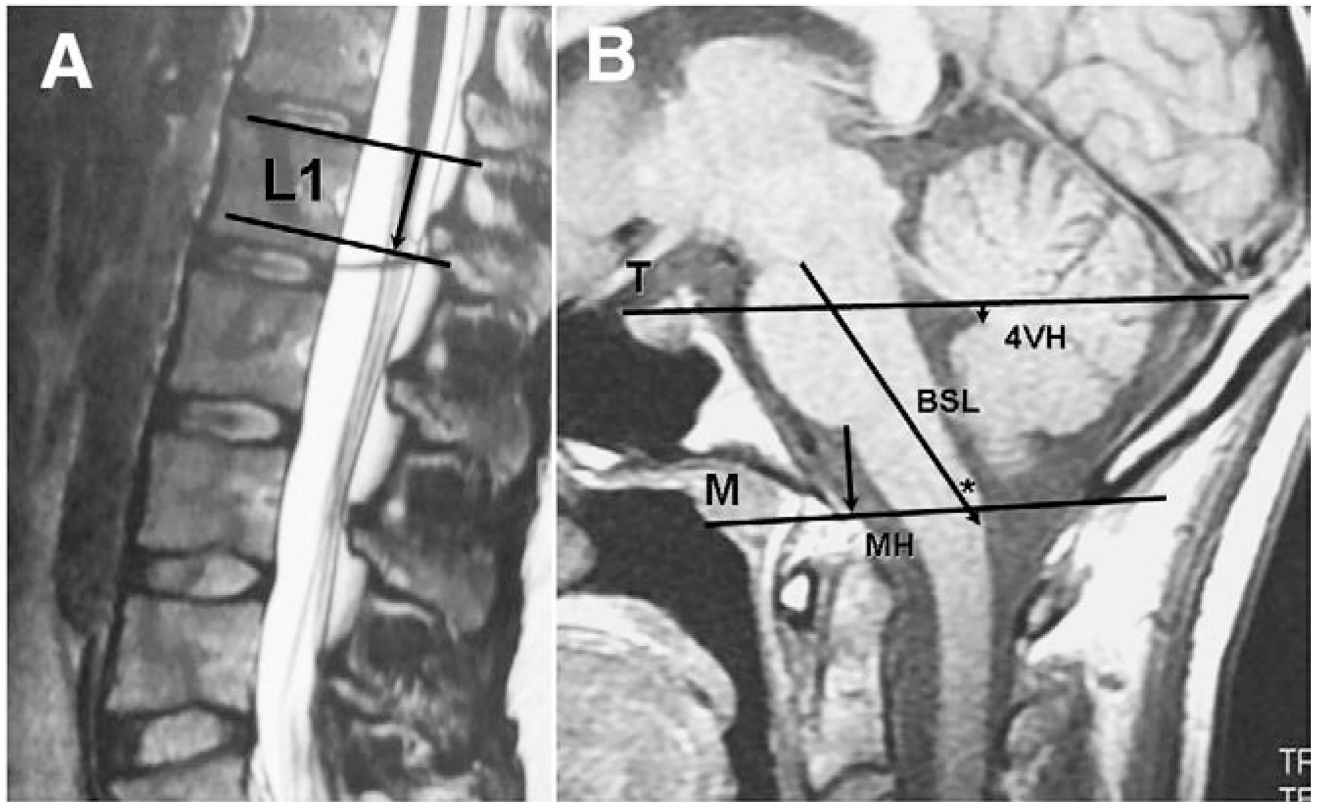


Fig. 1. Lines and measurement intervals for assessing neural and osseous structures at the TLJ and CCJ in 25-year-old healthy control female. A: Midsagittal T2-weighted MR image of lumbar spine showing position of CMD measured as distance between upper endplate of L₁ (upper line) and tip of CMD (lower line). B: Midsagittal T1-weighted MR image of PCF showing Twining's line (T) between internal occipital protuberance and tuberculum sellae and McRae's line (M) between opisthion and basion.

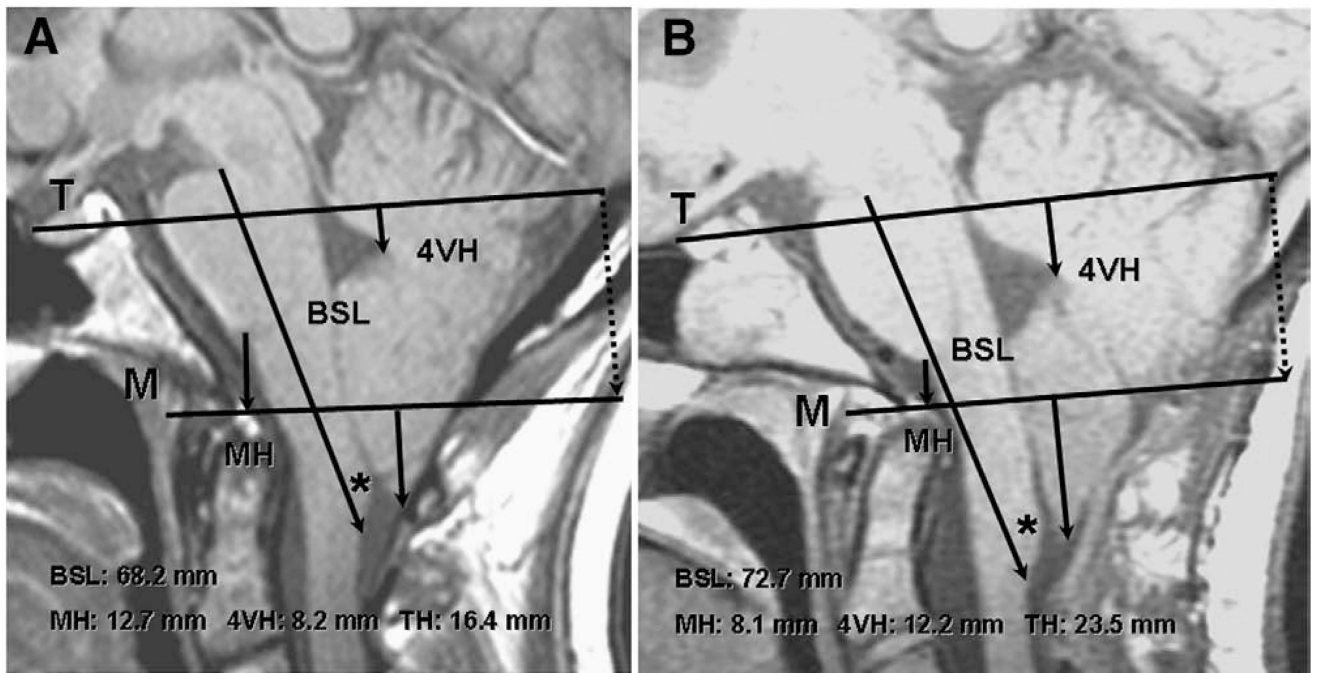


Fig. 2.

Morphometric assessments of CCJ in 24-year-old woman with CM-I/TCS before and after failed Chiari surgery. A: Preoperative midsagittal T1-weighted MR image showing elongation of brain stem (BSL = 68.2 mm), downward displacement of medulla (MH = 12.9 mm), downward displacement of cerebellum (4VH = 7.6 mm), and herniation of cerebellar tonsils (TH = 17.8 mm). To reconstruct line M on postoperative films, the distance between the internal occipital protuberance and line M was measured along a line drawn perpendicular to line T (dotted line). B: postoperative scan with reconstructed line M, 6 months after posterior fossa decompression showing cerebellar ptosis with greater elongation of brain stem (BSL = 72.7 mm), greater downward displacement of medulla (MH = 7.6 mm), greater downward displacement of cerebellum (4VH = 12.9 mm), and greater herniation of cerebellar tonsils (TH = 25.0 mm). Asterisk indicates gracile tubercle.

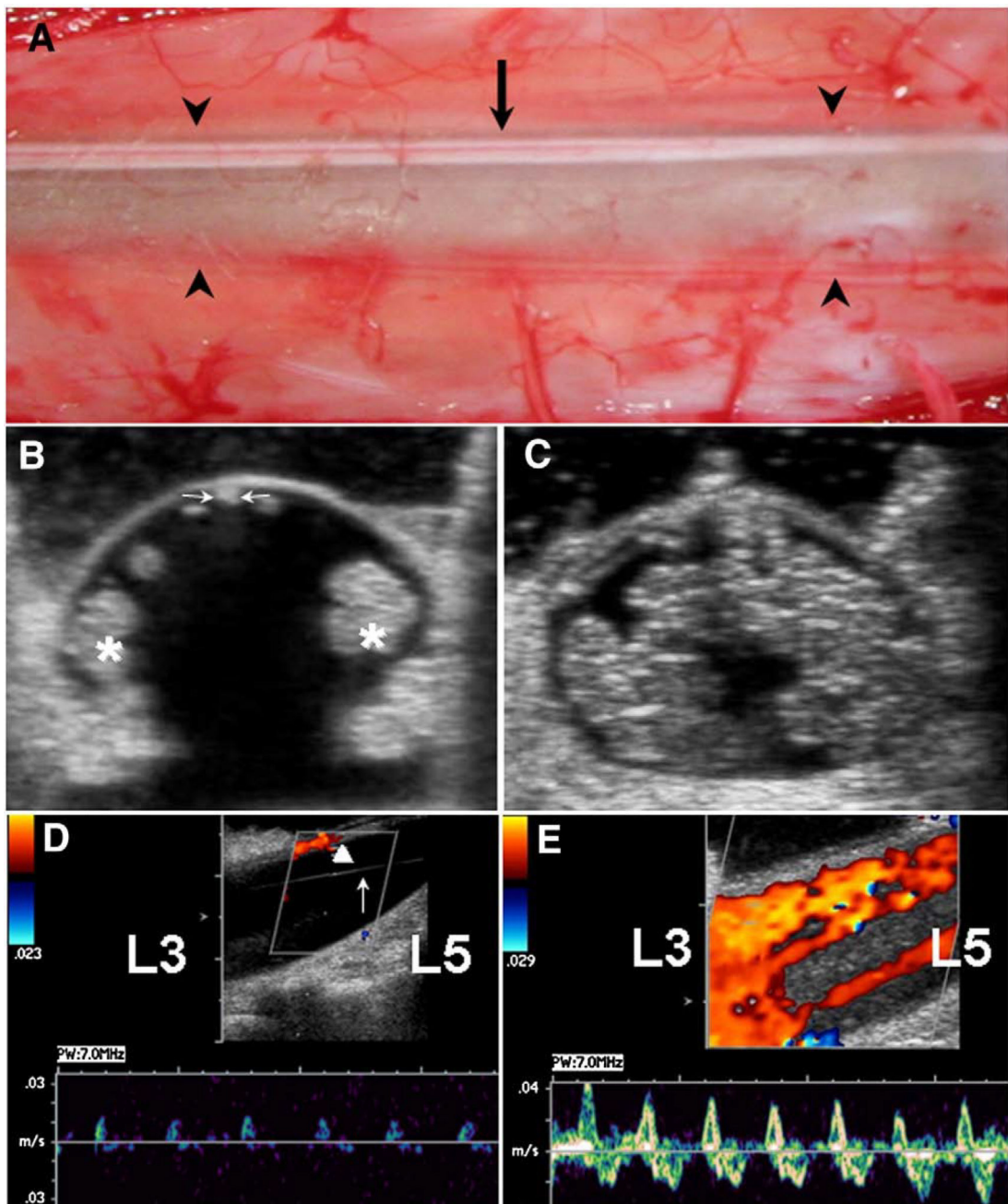


Fig. 3.

A: Intraoperative photograph of lumbar theca at L₄ in 46-year-old female with CM-I/TCS showing semitransparent dura with midline ectasia defined by arrowheads. Arrow identifies thin, taut, dorsally positioned FT. B-E: Intraoperative CDU assessments in 5-year-old male with CM-I/TCS. B: Axial image at L₄ before opening dura showing dorsal position of FT (arrow) and lateral packing of cauda equina roots (asterisks). The FT measures 0.8 mm in transverse diameter. C: Axial image at L₄ after SFT and closing dura showing even distribution of cauda equina roots. D: Midsagittal image at L₄ before opening dura showing 0.5 to 1.2 cm/s CSF flow with arterial pulsations, low power, and high resistance. Laterally

packed cauda equina roots are not visualized in midline plane. Arrow identifies stretched arachnoid band. Arrowhead identifies dorsally positioned FT. E: Midsagittal image at L₄ after SFT and closing dura showing 3.5 to 4.0 cm/s CSF flow in multiple streams with arterial, venous, and respiratory variations, bidirectional movement, high power, and reduced resistance.

Author Manuscript

Author Manuscript

Author Manuscript

Author Manuscript

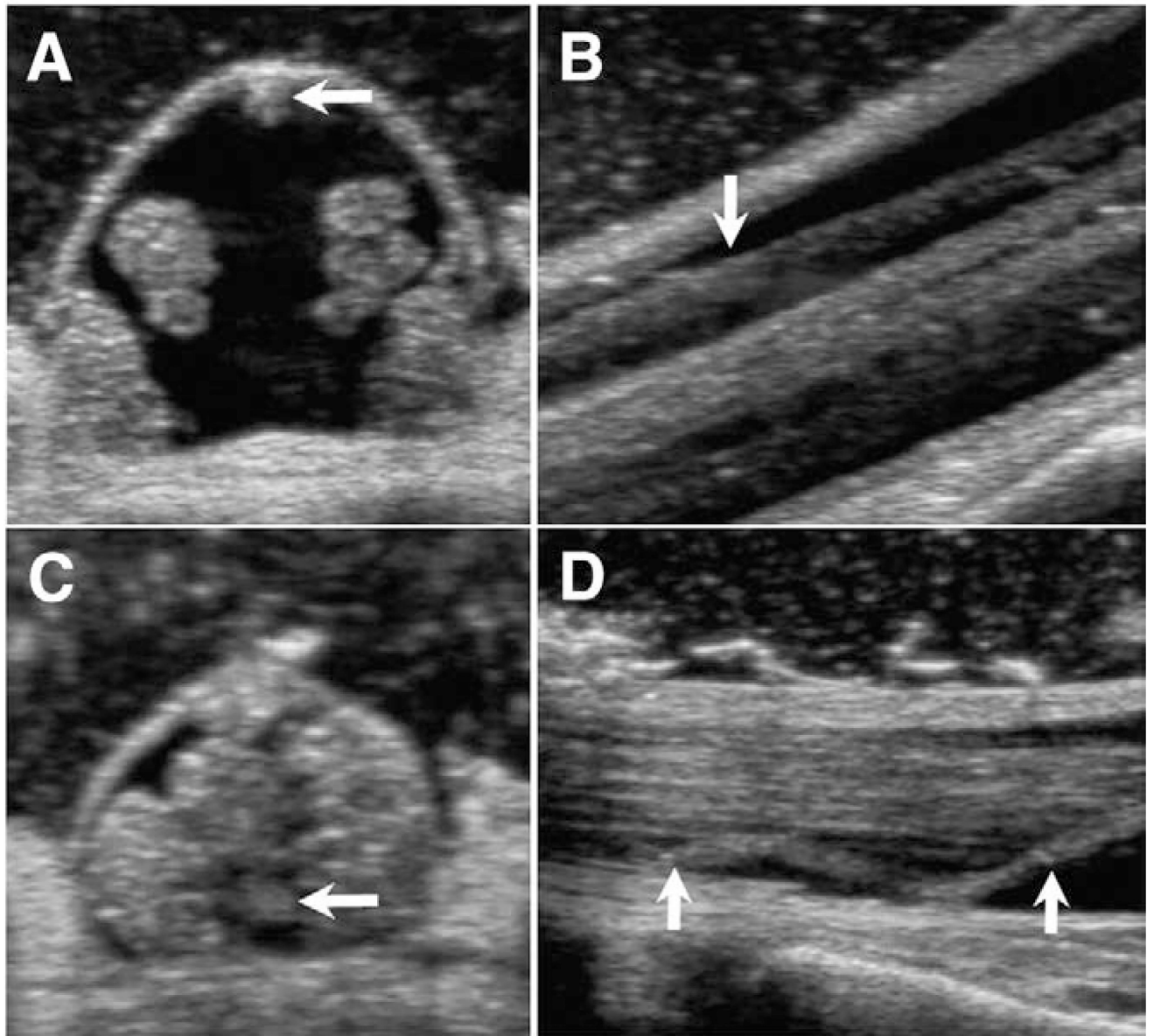


Fig. 4. Intraoperative CDU images before and after SFT in 33-year-old woman with CM-I/TCS. A: Axial image at L₄ before opening dura showing posterior position of FT (arrow) and lateral packing of cauda equina roots. B: Sagittal image at L₄ before opening dura. Arrow points to posteriorly positioned FT. C: Axial image at L₄ after SFT and closing dura showing anterior position of sectioned FT (arrow) and even distribution of cauda equina roots. D: Sagittal image at L₄ after SFT and closing dura showing limp proximal end of sectioned FT (arrows) in ventral subarachnoid space.



Fig. 5.
Midsagittal T1-weighted MR images of thoracic spine in 36-year-old man with CM-I/TCS.
A: Preoperative scan showing T₇ to T₉ syringomyelia. B: Postoperative scan 6 months after SFT showing reduction in syrinx size.

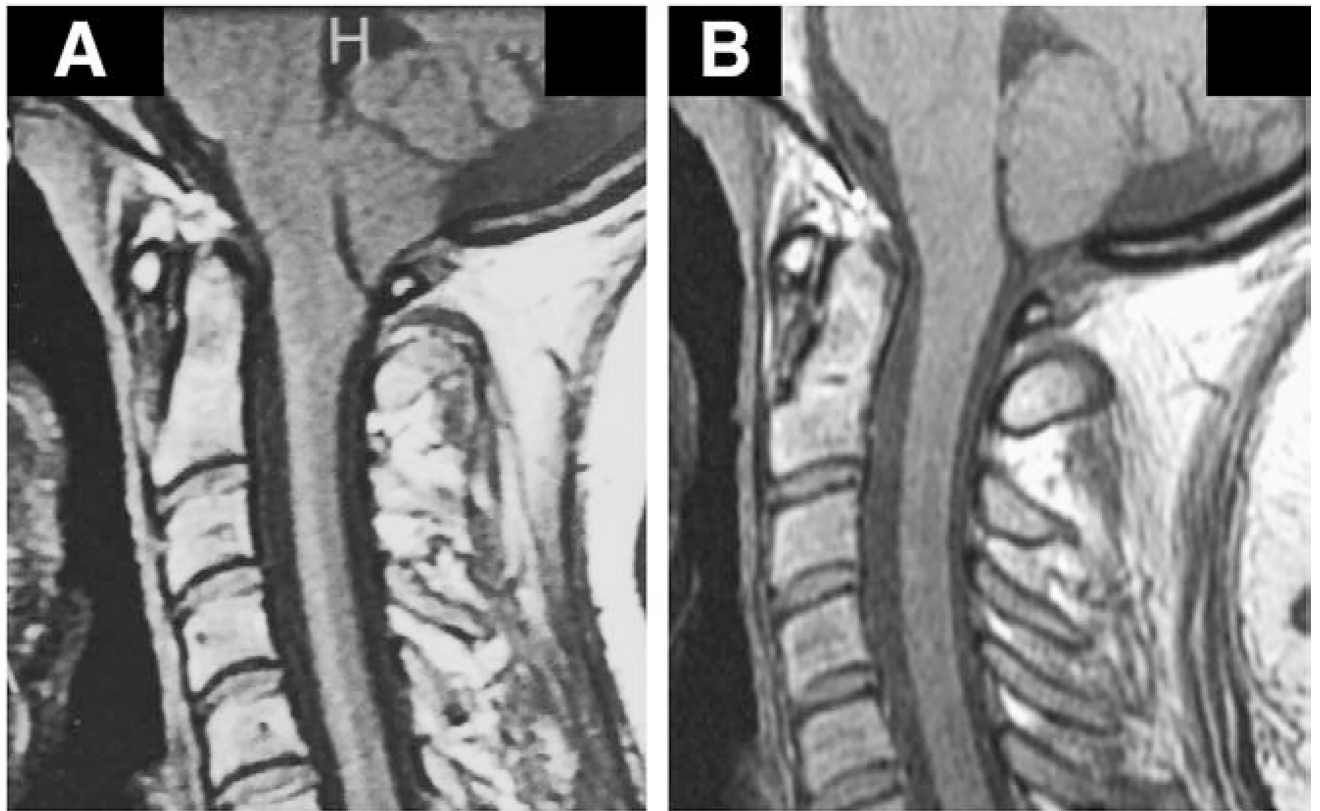


Fig. 6. Midsagittal T1-weighted MR images before and after SFT in 28-year-old woman with CM-I/TCS. A: Preoperative scan showing tonsillar herniation extending to superior arch of C₁. Morphometric measurements revealed elongation of brain stem (BSL = 60.1 mm), downward displacement of medulla (MH 7.7 mm), downward displacement of cerebellum (4VH = 14.4 mm), herniation of cerebellar tonsils (TH = 12.3 mm), and enlargement of FM (transverse diameter = 34.3 mm). B: Postoperative scan 7 months after SFT showing resolution of CM-I. Morphometric measurements revealed normalization of brain stem length (BSL = 53.7 mm), resolution of hindbrain displacement (MH = 12.4, 4 VH = 4.0 mm), and ascent of cerebellar tonsils (TH = 1.5 mm).

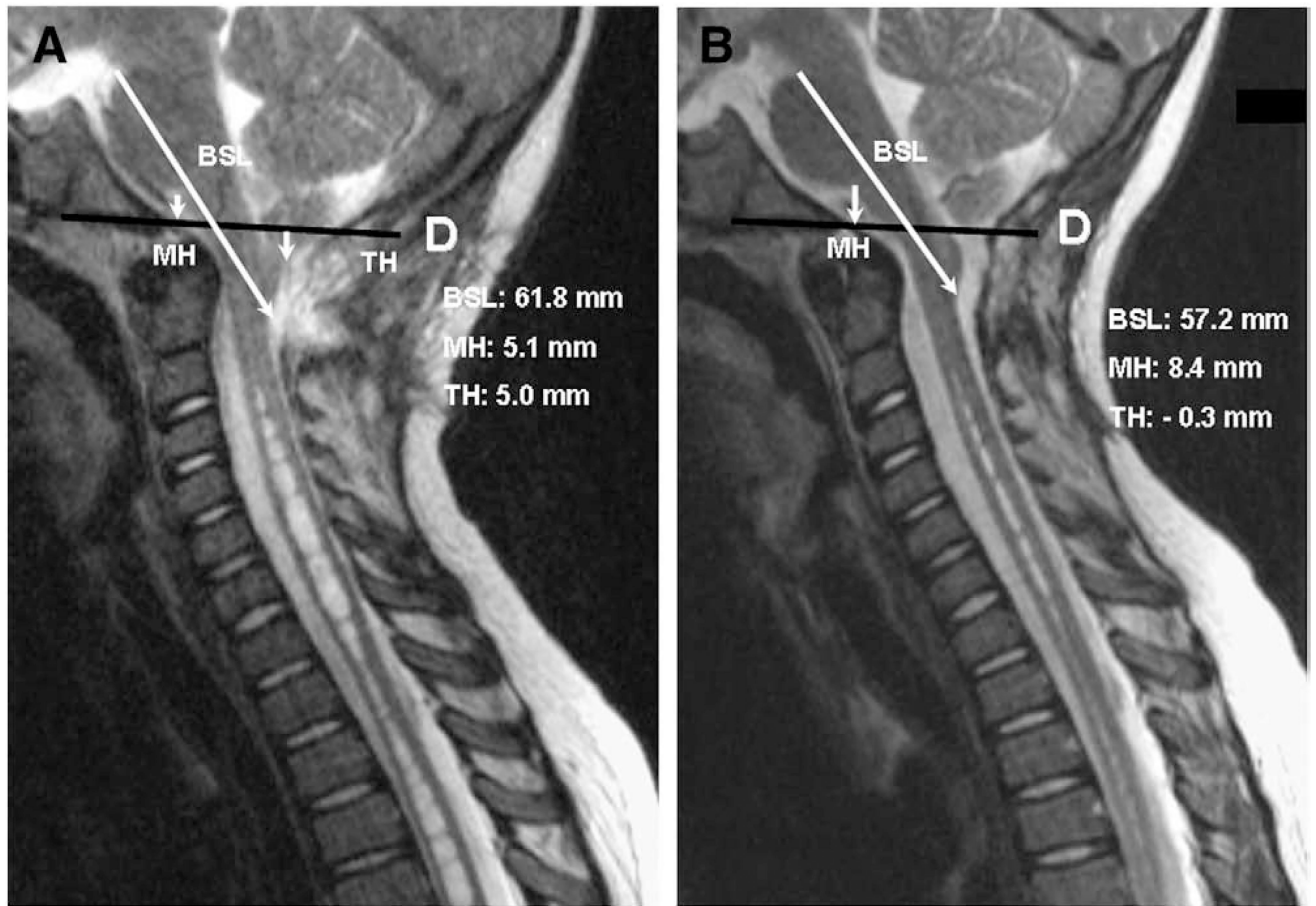


Fig. 7. Morphometric measurements of CCJ before and after SFT in 8-year-old female with CM-I/TCS and slowly progressive syringomyelia 3 years after Chiari decompression surgery had failed to reduce syrinx size. Reconstructed CT scans of head revealed complete reossification of suboccipital craniectomy. A: Midsagittal T-2 weighted MR image before SFT showing elongation of brain stem (BSL = 61.8 mm), downward displacement of medulla (MH = 5.1 mm), herniation of cerebellar tonsils (TH = 5.7 mm), and persistent cervicothoracic syringomyelia. B: Postoperative scan 5 weeks after SFT showing reduction of BSL (57.2 mm), ascent of medulla (MH = 7.4 mm), ascent of cerebellar tonsils (TH = 0), expansion of upper cervical subarachnoid spaces, and reduction in size of syringomyelia.

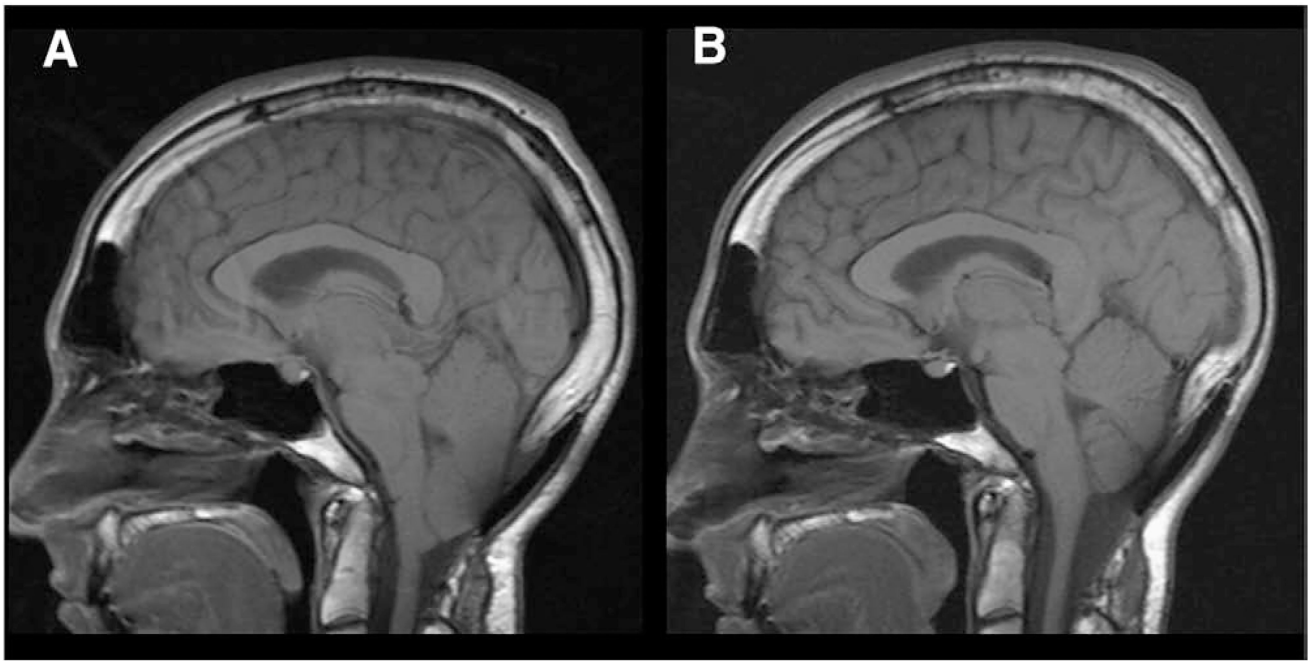


Fig. 8. Midsagittal T1-weighted MR images before and after SFT in 27-year-old man with CM-I/TCS who developed progressive cerebellar ptosis and recurrent Chiari symptoms after posterior fossa decompression. A subsequent cranioplasty 1 year before SFT failed to arrest ongoing prolapse and clinical deterioration. A: Preoperative scan showing suboccipital craniectomy, overlying cranioplasty plate, and cerebellar ptosis with elongation and downward displacement of hindbrain. The cerebellum is grossly misshapened and vertically oriented. Morphometric measurements confirmed elongation of brain stem (BSL = 61.7 mm), downward displacement of medulla (MH = 10.8 mm), and downward displacement of cerebellum (4VH = 28.7 mm). B: Postoperative scan 8 months after SFT showing resolution of cerebellar ptosis and anatomical remodeling of cerebellum. Morphometric measurements revealed normalization of brain stem length (BSL = 52.8 mm) with ascent of medulla (MH = 14.4 mm) and cerebellum (4 VH = 18.1 mm).

Table 1

Characteristics of patients with CM-I/TCS and LLCT/TCS undergoing SFT

Variable	Patient group (%)		
	CM-I/TCS	LLCT/TCS	Controls
Total no. of cases	280	38	155
Age (y)			
0–3	5 (2)	2 (5)	20
4–7	17 (6)	1 (3)	20
8–11	15 (5)	2 (5)	20
12–15	15 (5)	3 (8)	20
16–18	11 (4)	3 (8)	20
19 – 69	217 (78)	27 (71)	55
Sex			
Male	47 (17)	14 (37)	30
Female	233 (83)	24 (63)	125
Failed Chiari surgery	131 (34)	22 (58)	

Numbers in parentheses denote percentages.

Author Manuscript

Author Manuscript

Author Manuscript

Author Manuscript

Table 2

Clinical presentation of 318 patients undergoing SFT

Variables	Patient Group (%)	
	Children	Adults
Total no. patients	74 (12)	244 (88)
Symptoms and signs related to TH		
Suboccipital headache	61 (82)	221 (90)
Posterior neck pain	58 (78)	197 (81)
Dizziness	44 (60)	163 (67)
Nausea and vomiting	36 (49)	118 (48)
Symptoms and signs related to TCS		
Low back pain	57 (77) **	220 (90) **
Leg pain	60 (82)	201 (82)
Urinary urgency or incontinence	69 (93) **	177 (73) **
Lower extremity numbness or motor weakness	52 (70)	176 (72)
Muscular atrophy	14 (19)	62 (25)
Bowel disturbances	47 (64)	166 (68)
Numbness of pelvic area	28 (38) ***	169 (69) ***
Positive FT traction tests ^a	56 (76)	169 (69)
Miscellaneous symptoms and signs		
ADHD	17 (23)	3 (1)
Interscapular pain	5 (7) ***	78 (32) ***
Paraesthesias hands/feet	24 (32) **	123 (50) **
Diagnostic findings		
Tonsillar descent below FM		
0–4 mm (low-lying tonsils)	11 (15)	27 (11)
5–7 mm (minimal tonsillar herniation)	15 (20) **	99 (41) **
8–32 mm	48 (65) *	118 (48) *
Syringomyelia		
Terminal syrinx (below T5)	23 (31)	54 (22)
Cervicothoracic syrinx	10 (14)	33 (14)
Holocord syrinx	8 (11)	10 (4)
Thoracolumbar scoliosis	24 (32) *	47 (19) *
Lumbarization of S1	8 (11)	18 (7)
Position of CMD		
Above lower endplate L2	60 (81) ***	240 (98) ***
Below lower endplate L2	14 (19) ***	4 (2) ***
Spina bifida occulta	9 (12)	18 (7)
Neurogenic bladder (urodynamics)	56 (76) ***	131 (53) ***
Failed Chiari surgery		

Variables	Patient Group (%)	
	Children	Adults
Total no. of patients	19 (26)	134 (55)
Cerebellar prolapse	13 (67)	83 (62)
Cerebellar hernia	7 (37)	44 (32)

Numbers in parentheses denote percentages.

^aToe walking, heel walking, and pelvic traction tests.

* Significant differences between children and adults ($P < .05$).

** Significant differences between children and adults ($P < .01$).

*** Significant differences between children and adults ($P < .001$).

Table 3

Comparison of morphometric measurements and volumetric calculations in patients with CM-I, CM-I/TCS, and LLCT/TCS

Variable	Normal controls	CM-I	CM-I/TCS	LLCT/TCS
Total no. of patients	75	280	228	30
Sex (male/female)	20 / 55	78 / 202	40 / 188	12 / 18
Mean age (y)	31.7 ± 11.8	33.7 ± 10.4	31.5 ± 12.4	31.0 ± 12.5
Brain structures				
BSL (mm)	51.6 ± 2.32	52.1 ± 2.57	57.5 ± 2.22 [*] , [‡]	54.8 ± 2.28 [*]
TH (mm)	-3.4 ± 2.71	11.5 ± 4.41 [*]	8.4 ± 2.45 [*]	3.5 ± 1.04 [*]
4VH ^a (mm)	4.2 ± 3.14	5.1 ± 3.13	8.1 ± 2.27 [*] , [‡]	5.2 ± 2.32 [*]
Occipital bone size				
Clivus				
Axial length (mm)	47.0 ± 2.17	38.4 ± 3.21 [†]	45.7 ± 2.85	46.3 ± 2.87
Supraocciput				
Axial length (mm)	47.7 ± 2.52	39.7 ± 3.87 [†]	47.0 ± 2.77	47.4 ± 2.56
Occipital condyle				
Axial length right (mm)	24.1 ± 1.65	18.7 ± 3.40 [†]	23.3 ± 2.61	23.8 ± 2.71
Axial length left (mm)	24.3 ± 1.54	19.1 ± 3.56 [†]	23.5 ± 2.78	23.9 ± 2.83
Width between occipital condyles (mm)	50.5 ± 2.48	47.2 ± 3.12 [†]	55.2 ± 3.34 [*]	54.1 ± 2.74 [*]
FM				
Anterior-posterior diameter (mm)	32.1 ± 3.17	32.8 ± 3.72	37.6 ± 2.56 [*] , [‡]	35.0 ± 2.54 [*]
Transverse diameter (mm)	29.6 ± 3.74	26.1 ± 3.04 [†]	34.8 ± 3.28 [*]	33.6 ± 3.15 [*]
Area (mm ²)	787.7 ± 118.4	655.7 ± 121.8 [†]	1028.5 ± 122.8 [*]	923.2 ± 120.8 [*]
Volumetric analysis				
PCFV (ml)	189.1 ± 7.84	164.6 ± 8.17 [†]	186.2 ± 8.60	188.7 ± 8.64
PFBV (ml)	151.8 ± 3.14	148.7 ± 4.76	152.8 ± 4.46	152.7 ± 4.31
CSF space (ml)	37.2 ± 5.57	15.8 ± 8.41 [†]	33.4 ± 4.71	35.8 ± 4.57

Mean values are expressed as ± SDs.

^aDistance between Twining's line and posterior apex of fourth ventricle.

^{*}Significant differences (larger) as compared to normal controls ($P < .001$).

[†]Significant differences (smaller) as compared to normal controls ($P < .001$).

[‡]Significant differences (larger) as compared to LLCT/TCS group ($P < .01$).

Table 4

Preoperative morphometric analysis of TLJ and CCJ in patients undergoing SFT

Variable	No.	CMD ^a (mm)	BSL (mm)	MH (mm)	TH (mm)	4VH ^b (mm)
Total no. of patients	318					
Patient group by age (y)						
0–3						
Patients	7	28.2 ± 8.86	62.5 ± 3.57	7.1 ± 1.87	14.2 ± 4.25	2.5 ± 2.41
Healthy controls	20	23.2 ± 5.54	42.8 ± 2.77	12.4 ± 2.12	-3.7 ± 2.25	-0.7 ± 2.44
<i>P</i>		<i>P</i> < .01	<i>P</i> < .005	<i>P</i> < .005	<i>P</i> < .005	<i>P</i> < .005
4–7						
Patients	18	28.4 ± 7.31	58.7 ± 2.01	9.6 ± 2.23	9.7 ± 3.96	3.2 ± 3.58
Healthy controls	20	22.9 ± 6.68	45.4 ± 3.52	14.8 ± 3.35	-2.4 ± 2.51	2.4 ± 3.21
<i>P</i>		<i>P</i> < .01	<i>P</i> < .001	<i>P</i> < .001	<i>P</i> < .001	<i>c</i>
8–11						
Patients	17	27.9 ± 11.49	57.6 ± 1.84	12.0 ± 2.58	8.2 ± 2.44	5.5 ± 3.27
Healthy controls	20	20.2 ± 7.27	48.7 ± 2.45	16.1 ± 4.42	-3.0 ± 3.52	3.2 ± 2.76
<i>P</i>		<i>c</i>	<i>P</i> < .001	<i>P</i> < .001	<i>P</i> < .001	<i>P</i> < .01
12–15						
Patients	18	25.4 ± 11.72	57.4 ± 2.42	13.4 ± 3.72	7.4 ± 5.17	7.2 ± 3.85
Healthy controls	20	18.8 ± 6.65	50.2 ± 2.54	17.5 ± 3.38	-2.8 ± 3.24	3.6 ± 2.97
<i>P</i>		<i>c</i>	<i>P</i> < .001	<i>P</i> < .001	<i>P</i> < .001	<i>P</i> < .001
16–18						
Patients	14	22.5 ± 12.41	57.8 ± 2.18	11.7 ± 2.43	7.5 ± 4.62	7.4 ± 3.34
Healthy controls	20	17.1 ± 8.82	51.4 ± 2.35	18.1 ± 4.55	-3.2 ± 3.65	4.1 ± 3.58
<i>P</i>		<i>c</i>	<i>P</i> < .001	<i>P</i> < .001	<i>P</i> < .001	<i>P</i> < .001
19–69						
Patients	244	21.2 ± 11.82	57.2 ± 2.23	12.5 ± 3.17	7.8 ± 3.54	7.8 ± 3.28
Healthy controls	55	15.7 ± 7.78	51.7 ± 2.31	18.7 ± 3.45	-3.5 ± 3.78	4.2 ± 3.72
<i>P</i>		<i>c</i>	<i>P</i> < .001	<i>P</i> < .001	<i>P</i> < .001	<i>P</i> < .001
All patients	318	22.6 ± 11.55	57.5 ± 2.87	12.2 ± 3.08	8.0 ± 3.70	7.3 ± 3.32
All healthy controls	155	18.9 ± 7.32	49.2 ± 2.61	16.8 ± 3.71	-3.2 ± 3.33	3.1 ± 3.27

Variable	No.	CMD ^a (mm)	BSL (mm)	MH (mm)	TH (mm)	4VH ^b (mm)
<i>P</i>	<i>c</i>	<i>P</i> < .001	<i>P</i> < .001	<i>P</i> < .001	<i>P</i> < .001	<i>P</i> < .001

Mean values are expressed as \pm SDs.

^aDistance between tip of CMD and upper endplate of L1 vertebral body.

^bDistance between Twining's line and posterior apex of fourth ventricle.

^cNo significant differences between patients with CM-I/TCS and healthy control individuals.

Table 5

Surgical outcome of 318 patients undergoing SFT

Variables	Patient Group (%)	
	Children	Adults
Total no. patients	74 (12)	244 (88)
Complications		
Total no. patients	2 (1)	7 (3)
Wound infection	0	3 (1)
CSF leak	0	2 (1)
Spinal instability	0	1
Epidural hematoma	0	1
Retethering	2 (1)	0
Symptoms and signs		
Resolved	27 (36) *	44 (18) *
Improved	42 (57)	159 (65)
Unchanged	5 (7)	39 (16)
Worse	0	2 (1)
Terminal thoracic syrinx (below T4)		
Total no. cases	23	54
Resolved	15 (65) *	15 (28) *
Smaller	5 (22)	20 (37)
Unchanged	3 (13)	19 (35)
Cervicothoracic syringomyelia		
Total no. of cases	10	33
Resolved	0	0
Smaller	6 (60) †	9 (27) †
Unchanged	4 (40) †	24 (73) †
Holocord syringomyelia		
Total no. of cases	8	10
Resolved	0	0
Smaller	3 (38)	3 (30)
Unchanged	5 (63)	7 (70)
Thoracolumbar scoliosis		
Total no. of cases	24	47
Resolved	5 (21)	0
Improved	11 (46) *	11 (23) *
Unchanged	8 (33) *	36 (77) *
Neurogenic bladder		
Total no. of cases	56	131
Resolved	37 (66) *	22 (17) *

Variables	Patient Group (%)	
	Children	Adults
Improved	15 (27) *	88 (67) *
Unchanged	4 (7)	21 (16)
Mean follow-up (months)	14.8 ± 4.38	16.5 ± 5.04

Numbers in parentheses denote percentages. Mean values expressed as ± SDs.

* Significant differences between children and adults ($P < .001$).

† Significant differences between children and adults ($P < .01$).

Author Manuscript

Author Manuscript

Author Manuscript

Author Manuscript

Table 6

Postoperative morphometric analyses of TLJ and CCJ in patients undergoing SFT

Variable	No.	CMD ^a (mm)	BSL (mm)	MH (mm)	TH (mm)	4VH ^b (mm)
Total no. of patients	318					
Patient groups by age (y)						
0-3	7	20.5 ± 8.81	55.8 ± 3.07	10.4 ± 1.34	8.6 ± 3.70	0.5 ± 3.14
4-7	18	22.7 ± 7.62	52.7 ± 1.42	12.7 ± 1.36	5.2 ± 2.86	2.4 ± 2.73
8-11	17	22.8 ± 11.28	52.2 ± 1.96	14.4 ± 1.23	5.5 ± 2.60	3.5 ± 3.36
12-15	18	20.2 ± 11.65	52.5 ± 2.14	17.2 ± 2.40	4.5 ± 4.17	4.2 ± 3.37
16-18	14	17.8 ± 12.85	54.1 ± 1.51	15.1 ± 1.74	4.0 ± 3.24	4.8 ± 3.52
19-60	244	16.4 ± 11.77	53.7 ± 1.55	15.8 ± 2.11	4.0 ± 2.37	5.1 ± 4.57
All patients	318	17.5 ± 11.53	53.6 ± 1.65	15.5 ± 2.02	4.2 ± 2.57	4.7 ± 4.30

Mean values expressed as ±SDs.

^aDistance between upper endplate of L1 and CMD.

^bDistance between Twining's line and posterior apex of fourth ventricle.